Biomacromolecules

pubs.acs.org/Biomac

Article

Harvesting Far-Red Light with Plant Antenna Complexes Incorporating Chlorophyll *d*

Eduard Elias,[§] Nicoletta Liguori,[§] Yoshitaka Saga, Judith Schäfers, and Roberta Croce*

Cite This: *Biomacromolecules* 2021, 22, 3313−3322

Read Online

ACCESS | Metrics & More | Article Recommendations | Supporting Information

ABSTRACT: Increasing the absorption cross section of plants by introducing far-red absorbing chlorophylls (Chls) has been proposed as a strategy to boost crop yields. To make this strategy effective, these Chls should bind to the photosynthetic complexes without altering their functional architecture. To investigate if plant-specific antenna complexes can provide the protein scaffold to accommodate these Chls, we have reconstituted the main light-harvesting complex (LHC) of plants LHCII *in vitro* and *in silico*, with Chl *d*. The results demonstrate that LHCII can bind Chl *d* in a number of binding sites, shifting the maximum absorption ∼25 nm toward the red with respect to the wild-type complex (LHCII with Chl *a* and *b*) while maintaining the native LHC architecture. Ultrafast spectroscopic measurements show that the complex is functional in light harvesting and excitation energy transfer. Overall, we here demonstrate that it is possible to obtain plant LHCs with enhanced far-red absorption and intact functional properties.

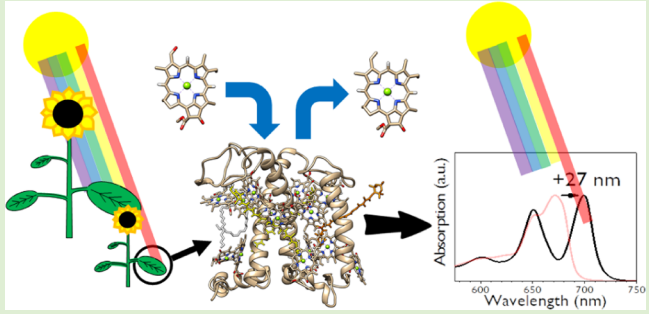

INTRODUCTION

In plants, solar energy is predominantly captured by the light-harvesting complexes (LHCs), which are membrane-spanning pigment−protein complexes binding Chl *a*, Chl *b*, and carotenoids (Cars). LHCs absorb photons in the visible range of the solar spectrum and efficiently transfer the excitation energy to the reaction centers of photosystems II and I (PSII and PSI), where charge separation occurs. The absorption cross section of the LHCs poses a limit to the light-harvesting capacity of crop canopies when plants are located very close to each other:[1,2] leaves at the top of the canopy tend to absorb the large majority of visible photons, thereby shading the lower leaves, which receive too little visible photons to perform photosynthesis optimally.[3] However, the light at the bottom of a canopy still contains some green photons and is rich in far-red and near-infrared photons (λ > 700 nm) (see Figure 1A).[3] Expanding the absorption cross section of plants toward these spectral regions represents a promising strategy for optimizing light usage in crops and, possibly, for increasing biomass yield.[3]

Recently, efforts have been conducted to increase the absorption cross section of plant LHCs by the addition of artificial dyes (see e.g., refs 6−8). The covalent attachment of rhodamine red to LHCII was shown to functionally increase the absorption of the complex in the green (λ = 500−600 nm).[6] Similarly, the organic dye Texas red was incorporated into liposomes containing LHCIIs, increasing the absorption of green light.[7] Finally, the association of an organic boron dye with LHCII resulted in a complex with enhanced absorption in the near infrared.[8] However, a limit of all these approaches is that the organic dyes cannot be naturally synthesized by photosynthetic organisms, limiting their future applications.

The recent discovery of far-red light photoacclimation cyanobacteria, in which the red-shifted Chls *d* and *f* are incorporated into the photosystems,[9,10] has sparked interest in introducing these Chls into plants.[2,3,11] Indeed, it is estimated that through the absorption of far-red light, a gain of 19% in photosynthetic efficiency could be achieved.[11] It has been proposed that in these so-called "smart canopies", the production and incorporation of red-shifted Chls could be phytochrome-regulated,[3] allowing for a rational penetration across the canopy of the different light colors.

Chl *d* is the principal light absorber in *Acaryochloris marina*, which uses far-red photons to perform photochemistry with an efficiency that is similar to that of plants.[12] Moreover, it has been shown that Chl *d* can perform nearly all functions that Chl *a* carries out in plant photosynthesis.[13] *In vivo* synthesis of Chl *d* in *A. marina* is thought to occur through a single enzymatic step taking Chl *a* as a precursor,[14,15] potentially facilitating the design of plants that synthesize Chl *d*, when the enzyme responsible for the reaction will be identified. Structurally, Chl *d* differs from Chl *a* only in the C-3 position

Received: April 2, 2021
Revised: June 28, 2021
Published: July 16, 2021

https://doi.org/10.1021/acs.biomac.1c00435
Biomacromolecules 2021, 22, 3313−3322

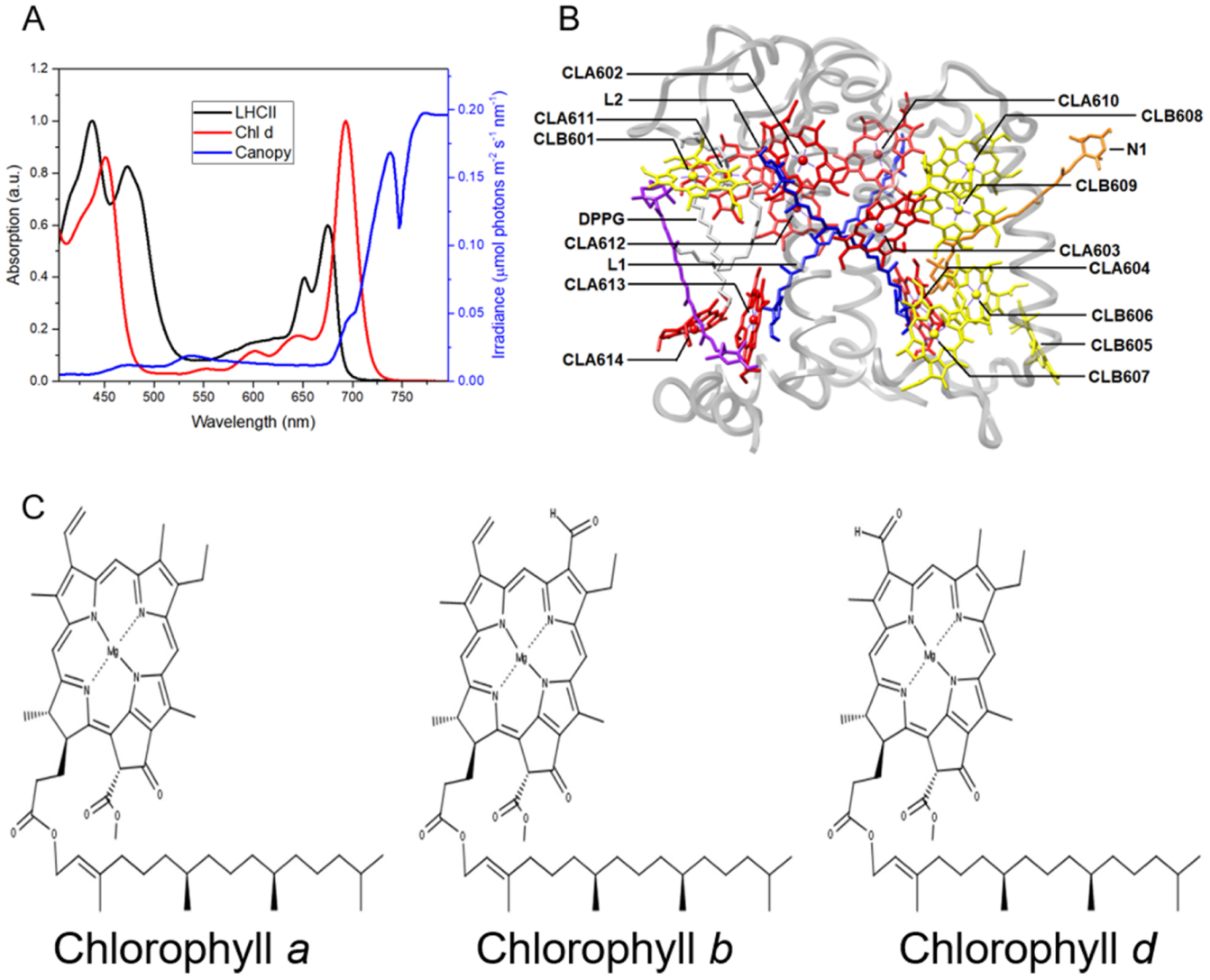

Figure 1. LHCII and chlorophylls. (A) Photon flux penetrating a dense canopy (digitized from ref 4), absorption spectrum of LHCII trimers, and of Chl *d* in 80% acetone. (B) Annotated LHCII structure with cofactors according to the crystal structure.[5] (C) Chemical structures of chlorophyll *a*, *b*, and *d*.

where a formyl group substitutes a vinyl group, and from Chl *b* only in the C-7 position where Chl *d* has a methyl group instead of a formyl group (see Figure 1C). Chl *d* might thus be able to bind to the LHC proteins. This assumption is supported by the fact that several of the Chl binding sites in plant LHCs are promiscuous, being able to accommodate both Chl *a* and *b*,[16−18] suggesting that at least some binding sites of LHCs are less selective and could be occupied by other Chl types. Indeed, it has been found that Chl *d* binds with a comparable affinity as Chl *a* to a peptide maquette containing a nine amino acid-long sequence that is identical to a segment of LHCII that contains the axial ligands for CLA602 and CLA603 (see Figure 1B for a structure of LHCII).[19,20]

To test if plant LHCs are indeed capable of binding Chl *d*, we reconstituted the major LHC of plants, LHCII, with a pigment mix in which Chl *a* was replaced by Chl *d*. *Via* a combination of biochemical analyses, spectroscopy, and molecular dynamics (MD) simulations, we verified the functional insertion of Chl *d* in LHCII and the effect of Chl *d* binding on the molecular architecture of the complex and its light-harvesting properties. All of the experimental and computational results on LHCII binding Chl *d* were here analyzed and compared with those of the native LHCII binding Chl *a* and *b* (indicated as LHCII-ab).

EXPERIMENTAL (MATERIALS AND METHODS)

Sample Preparation. LHCII reconstitutions were performed following the protocol described in ref 21. In short, LHCII inclusion bodies were obtained from the *Escherichia coli* host strain BL21 transformed with the Lhcb1 construct. Chl *a*, Chl *b*, and the native plant Cars were extracted from spinach. Chl *d* was extracted from *A. marina* cells as previously described.[22] For the reconstitution with Chl *d*, the pigment reconstitution mix was composed of 150 μg of Chl *d* (0.15 μmol), 100 μg of Chl *b* (0.10 μmol), and 60 μg of the Cars (0.10 μmol). For the control reconstitution, the reconstitution mix contained Chl *a* instead of Chl *d*. The reconstituted complexes were then further purified by affinity chromatography and sucrose density gradient ultracentrifugation in order to remove unbound pigments.

Steady-State Spectroscopy. Absorption spectra were acquired at room temperature on a Varian Cary 4000 UV−vis-spectrophotometer. Fluorescence emission and excitation spectra were measured at room temperature on a HORIBA Jobin-Yvon Fluorolog-3 spectrofluorometer at an OD $\ll$ 0.1 cm^{-1}. Circular dichroism (CD) spectra were taken on a Chirascan CD spectrophotometer at 10 °C at an OD of <1.0 cm^{-1}. For all the measurements, the sample

https://doi.org/10.1021/acs.biomac.1c00435
Biomacromolecules 2021, 22, 3313−3322

concentration was adjusted to the required OD with a buffer containing 10 mM HEPES (pH 7.5), 0.5 M sucrose, and 0.06% β-DM.

Pigment Composition Analysis. Pigments were extracted from the protein complexes in 80% acetone. The Chl *a*/*b*, Chl *b*/*d*, and Car/Chl ratios were estimated by fitting the absorption spectrum of the pigment extract with the spectra of the isolated pigments in the same solvent (Figure S1 in Supporting Information). The relative composition of the Cars was analyzed by HPLC. Further details about this combined approach are given in ref 23.

Time-Correlated Single-Photon Counting. Time-correlated single-photon counting measurements were performed at 10 °C using a FluoTime 200 (PicoQuant). The sample concentrations were adjusted to ≪0.1 cm^{-1} and measured in a 1 cm quartz cuvette. Excitation was provided at a 10 MHz repetition rate using a 468 nm laser diode (Chl *b* preferential excitation) at 10 μW. Emission was detected at the fluorescence peak wavelength for each sample, that is, at 680 nm for the LHCII-ab complex and at 704 nm for the LHCII-db complex. The instrument response function (IRF) was obtained by measuring the decay of a pinacyanol iodide dye dissolved in methanol, which has a 6 ps fluorescence lifetime.[24] Decay traces were fitted with a sequential model using the TRFA Data Processor Advanced software[25] (http://www.sstcenter.com).

Femtosecond Transient Absorption and Global Analysis. A mode-locked Ti:Sa oscillator (Coherent MIRA) in combination with a regenerative amplifier (Coherent Rega 9050) yielded pulses of approximately 70 fs at a repetition rate of 40 kHz at 800 nm. The beam from this laser system was consequently split with a ratio of 2:8 between a path for white-light continuum generation, achieved with a sapphire crystal (probe path) and one passing through an optical parametric amplifier (Coherent OPA 9400) tuned to a pump pulse color of 642 nm (pump path). The full width at half-maximum (fwhm) of the excitation pulses was reduced to 10 nm by means of interference filters (THORLABS), and the energy per pulse was set to 7.5 nJ. At this pulse energy, annihilation effects were not present, as evidenced by the absence of power dependence at the maximal bleach in the TA experiments (Figure S2A,B in Supporting Information). Both the probe and the pump pulses were intermittently turned off and on through the use of acousto-optic modulators (AA OPTO-ELETRONIC) triggered by a digital delay generator (Stanford Research Systems), allowing for active scatter and dark current correction. The polarization between the pump and probe pulse was set at the magic angle (54.7°). The white-light probe beam was dispersed and consequently detected on a charge-coupled device composed of 1024 pixels (Entwicklungsbüro EB Stresing), together covering a ∼240 nm spectral range. The time interval between the pump and probe was varied using a retroreflector mounted on a delay line, allowing us to record transient spectra up to 3.5 ns of delay between the pump and probe. The OD of the LHCII-db sample was adjusted to 2.6 cm^{-1} at its Q_y maximum, whereas for the LHCII-ab sample, this value was 1.6 cm^{-1}. The measurements were performed in a 1 mm-quartz cuvette. An oxygen scavenging system in the form of a mixture of glucose, glucose oxidase, and catalase was used for the measurement to prevent the formation of radical species and thereby sample degradation.[26] The sample cuvette was shaken throughout the measurement.

Global analysis[27] was performed using the Glotaran 1.5.1 software:[28] the raw two-dimensional TA data set was fitted to a noninteracting parallel kinetic scheme yielding the so-called decay associated difference spectra (DADS) and to a unidirectional sequential kinetic scheme yielding the evolution associated decay spectra (EADS). For a representation of the model used, see Figure 4A,D. In the formalism of the noninteracting parallel scheme, the TA data $\psi(\lambda,t)$ can be represented *via* the following function

$$\psi(\lambda, t) = \sum_{l=1}^{n} e^{-k_l * t} * \mathrm{DADS}_l(\lambda) \oplus \mathrm{IRF}(t)$$

In the model, k_l is an exponential decay rate associated with the spectral amplitude function, or $\mathrm{DADS}_l(\lambda)$, and $\mathrm{IRF}(t)$ is the IRF, which is convolved with each $\mathrm{DADS}_l(\lambda)$. Fitting the $\psi(\lambda,t)$ to a unidirectional sequential scheme ($\mathrm{EADS}_1 \rightarrow \mathrm{EADS}_2 \rightarrow \mathrm{EADS}_n$) returns instead the EADS, $\mathrm{EADS}_l(\lambda)$. $\mathrm{EADS}_l(\lambda)$ is the spectrum of the species l that decays exponentially into the following one (l + 1).

Absorption Spectrum Analysis. The absorption spectra of the recombinant samples were fitted in the Q_y-region (630−750 nm) with their constituent Chl absorption spectra in protein.[29] The absorption spectrum of Chl *d* in protein has not yet been determined experimentally. However, since the shape of the absorption spectra of Chl *a* and Chl *d* in the solvent in the Q_y-region are almost equivalent (80% acetone, Figure S3 the Supporting Information), we expect at least in first approximation the same behavior for the protein environment. We have therefore used the (shifted) spectrum of Chl *a* in protein to describe the spectrum of Chl *d*.

MD Simulations. Atomistic MD simulations in the microsecond range were performed using the GROMACS[30] 4.6.3 software. In total, six independent runs of a wild-type (WT) LHCII system with Chl *d* instead of Chl *a* in a solvated model membrane were performed. These simulations were compared to previously conducted simulations[31] on native LHCII (with Chl *a*) in the same model lipid membrane. The detailed protocol describing the forcefield, the generation of the input coordinates, the equilibration methodology, the MD settings, and the way the analyses were conducted are presented in text S1 in Supporting Information.

RESULTS AND DISCUSSION

Chl *d* Stably Binds to LHCII and It Is Functionally Connected to the Other Pigments. The complexes obtained from the reconstitution mixes containing Chl *b* and either Chl *d* or Chl *a* are referred to as LHCII-db and LHCII-ab, respectively. Chl *b* was used in all reconstitution mixes because it was previously shown to be essential for the folding of the complex.[18] Both the LHCII-ab and LHCII-db complexes migrated in the sucrose gradient in one well-defined band, which has the mobility of a monomeric LHC complex.

The pigment composition of the recombinant complexes is shown in Table 1. The Chl/Car ratio in the two complexes is very similar, suggesting that they bind the same number of Chls. Normalization to the sum of lutein and violaxanthin, which in monomeric LHCII are only accommodated in the two central sites,[16] indicates the presence of ∼12 Chls in each complex, in agreement with previous results.[16,18] LHCII-db binds more than six Chls *b* per monomer, suggesting that the Chl *b* specific binding sites of WT LHCII are occupied by Chl *b* also in this complex. LHCII-db binds five Chls *d*, meaning that Chl *d* occupies all the Chl *a* binding sites of LHCII-ab but one (Table 1). Considering that the Chl *a*/*b* ratio of the pigment mix used for the reconstitution of LHCII-ab was similar to the Chl *d*/*b* ratio used for LHCII-db (see the methods), it is likely that there is at least one Chl binding

Table 1. Pigment Composition of Complexes[a]

pigments	LHCII-db	LHCII-ab
Chl a		6.2 ± 0.1
Chl b	6.8 ± 0.1	5.8 ± 0.1
Chl d	4.8 ± 0.1	
Chl d/b−Chl a/b	0.7 ± 0.1	1.1 ± 0.0
Chl/Car	4.9 ± 0.1	5.7 ± 0.0
Lut	1.9 ± 0.1	2.0 ± 0.0
Vio	0.1 ± 0.0	0.0 ± 0.0
Neo	0.3 ± 0.1	0.2 ± 0.1

[a]Pigment content is normalized to the sum of Lut + Vio.

https://doi.org/10.1021/acs.biomac.1c00435
Biomacromolecules 2021, 22, 3313−3322

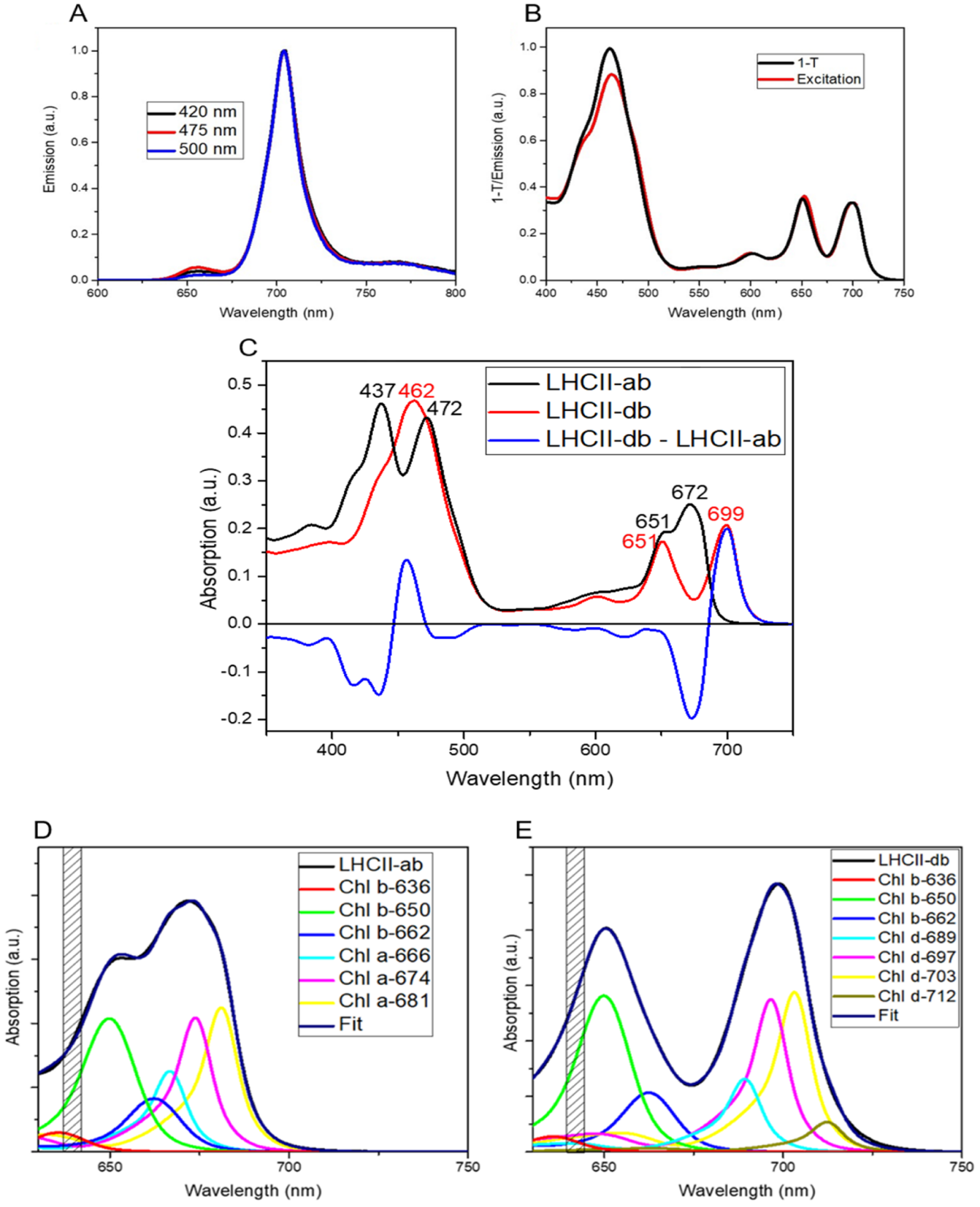

Figure 2. Chl *d* stably binds to LHCII and it is functionally connected to the other pigments. (A) Normalized fluorescence emission spectra of LHCII-db upon excitation at 420, 475, and 500 nm. (B) $1 - T$ *vs* fluorescence excitation spectrum of LHCII-db measured with emission at 704 nm. (C) Absorption spectra of LHCII-ab and LHCII-db normalized to their total Q_y absorption (λ = 630−750 nm) taking into account the pigment composition of each complex. (D) Deconvolution of LHCII-ab absorption spectrum. (E) Deconvolution of LHCII-db absorption spectrum. The excitation wavelength used for the TA experiments is indicated by the striped rectangles centered at 642 ± 5 nm.

https://doi.org/10.1021/acs.biomac.1c00435
Biomacromolecules 2021, 22, 3313−3322

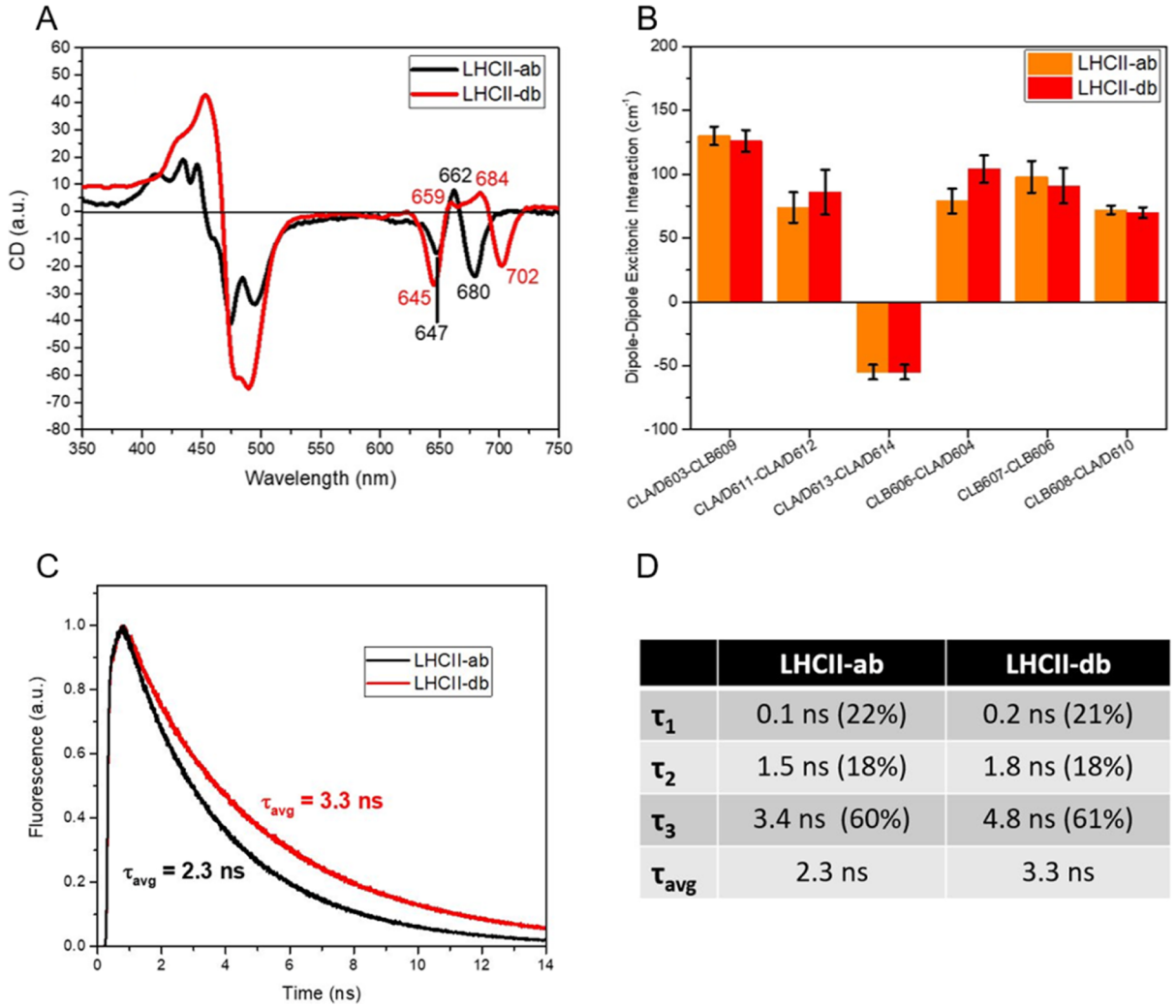

	LHCII-ab	LHCII-db
τ_1	0.1 ns (22%)	0.2 ns (21%)
τ_2	1.5 ns (18%)	1.8 ns (18%)
τ_3	3.4 ns (60%)	4.8 ns (61%)
τ_{avg}	2.3 ns	3.3 ns

Figure 3. LHCII-db maintains an excitonic architecture and is in a light-harvesting state. (A) CD spectra of LHCII-ab and LHCII-db scaled to the normalized Q_y peak of the corresponding absorption spectra. (B) Average excitonic interactions between the principal Chl pairs in the MD simulations. Data ± SE. Chl numbering as in ref 5 (see Figure 1B). (C) LHCII-ab and LHCII-db fluorescence decay after 468 nm excitation detected at the maximum of their steady-state emission spectra (680 and 704 nm, respectively). (D) Lifetime components and relative amplitudes (in brackets) obtained from global analysis.

pocket in LHCII, for which the binding affinity is Chl *a* > Chl *b* > Chl *d*.

To test whether the pigments bound to LHCII-db are all functionally connected, fluorescence emission was measured, and the resulting spectra are shown in Figure 2A. The emission spectra of the LHCII ab-complex are reported in Figure S4 in Supporting Information. Preferential excitation of either Chl *d*, Chl *b*, or the Cars at 420, 475, and 500 nm, respectively, resulted in very similar spectra, all peaking at 704 nm. This indicates that all the chromophores bound to LHCII-db are functionally connected and that the terminal emitter is a (cluster of) Chl *d*. A negligible fraction of disconnected Chl *b* is present, as indicated by the small emission peak at ∼655 nm. The functional connection of the pigments in LHCII-db is further confirmed by the good overlap between the 1-T and the excitation spectrum of the complex (Figure 2B).

Chl *d* Binding to LHCII Significantly Boosts the Absorption in the Far-Red. The absorption spectra of LHCII-ab and -db are reported in Figure 2C. The spectra are very similar in the Chl *b* Q_y absorption region, while the Q_y absorption maximum is shifted from 672 nm in LHCII-ab to 699 nm in LHCII-db. By fitting the Q_y region of the absorption spectra of LHCII-ab and LHCII-db with the spectra of their constituent Chls in the protein environment[29] (Figure 2D,E), we found that the Chl *b* spectra peak at the same wavelengths in both samples and have a very similar relative amplitude. This suggests that Chl *d* incorporation in LHCII does also not influence their spectral properties. The main Chl *a* and Chl *d* bands in LHCII-ab and LHCII-db are similarly shifted in energy and have comparable relative amplitudes. In LHCII-db, an additional small band was needed to fit the Chl *d* Q_y peak. This band probably compensates from the fact that we have used the same spectral shape for Chl *a* and *d* (corresponding to Chl *a* in protein[29]), while the spectrum of Chl *d* is probably slightly broader as in organic solvents (Figure S3 in Supporting Information).

Chl *d* Can Substitute for Chl *a* in LHCII. Maintaining the native folding of LHCII in the presence of Chl *d* is crucial in view of potential *in vivo* applications. Indeed, the conservation of the original protein and pigment architecture would ensure the correct assembly and functionality of LHCII-db in the PSII supercomplex. To investigate if the binding of Chl *d* in the Chl

https://doi.org/10.1021/acs.biomac.1c00435
Biomacromolecules 2021, 22, 3313−3322

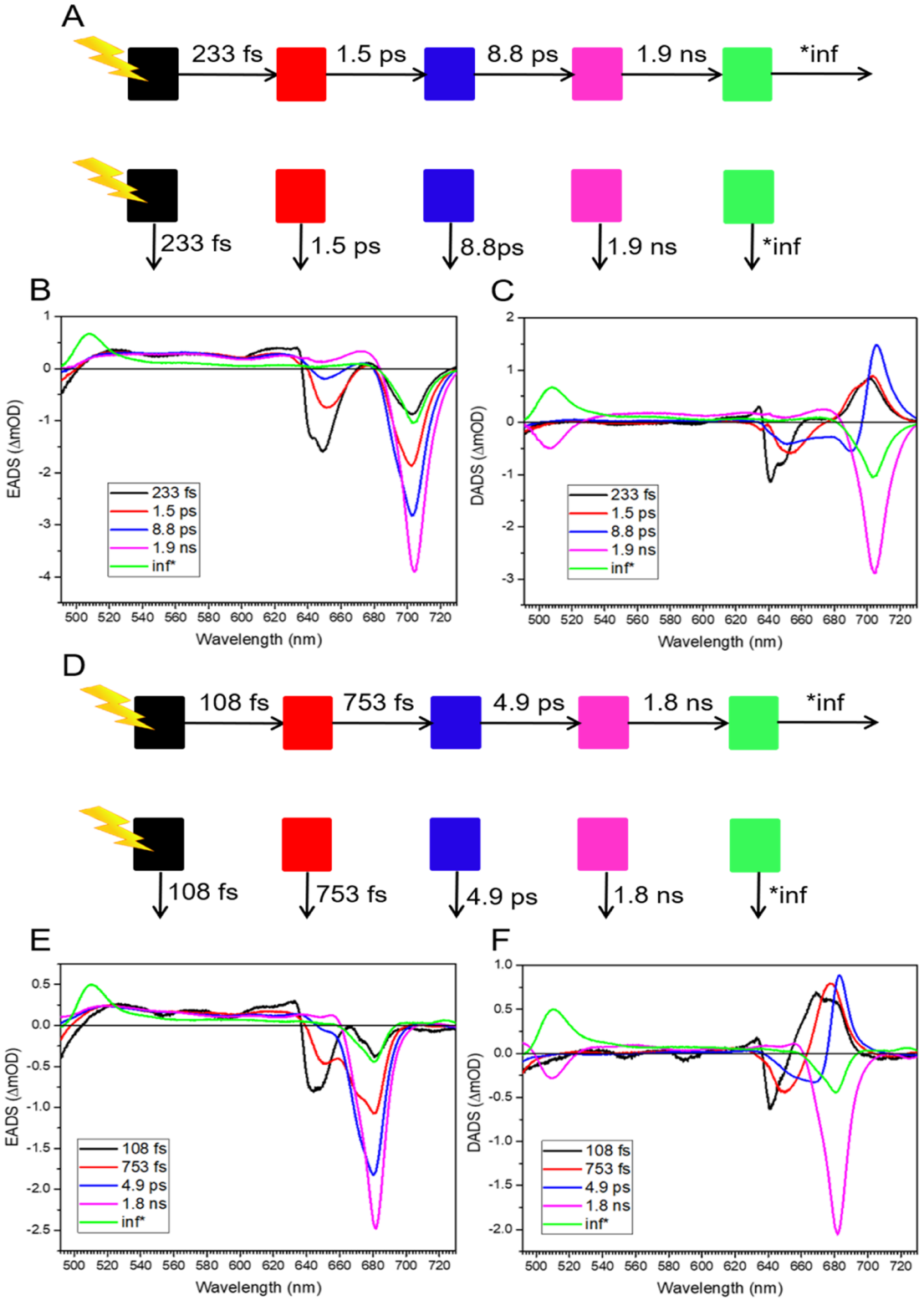

Figure 4. LHCII-db exhibits fast inter-Chl energy transfer. (A) Sequential (top) and parallel (bottom) models that were applied to the TA data set of the LHCII-db complex in the global analysis. (B) LHCII-db EADS arising from global analysis. (C) LHCII-db DADS arising from global analysis. (D) Sequential (top) and parallel (bottom) models that were applied to the TA data set of the LHCII-ab complex in the global analysis. (E) LHCII-ab EADS arising from global analysis. (F) LHCII-ab DADS arising from global analysis. * indicates a fixed lifetime in the fitting.

a binding sites of LHCII results in changes in the pigment and protein organization of the complex, we have performed several independent atomistic MD simulations of a monomer of LHCII-db. These simulations are compared to equivalent simulations of an LHCII-ab monomer.[31] The analyses were performed after the first 600 ns of each replica since at this stage, stabilization of the average RMSD of the C_α atoms of the protein occurs systematically (Figure S5A in Supporting Information). First, for the LHCII-db MD trajectories, we have computed the average distances between the central

https://doi.org/10.1021/acs.biomac.1c00435
Biomacromolecules 2021, 22, 3313−3322

magnesium of each Chls and its ligand and compared them to the LHCII-ab situation[31] (Figure S6B in Supporting Information). For all Chls, these distances only differ slightly between the two complexes, that is, maximally 0.21 ± 0.05 nm in the case of CLB605 and with an average difference of 0.06 ± 0.02 nm, indicating that there are no significant changes in the binding when Chl *a* or *d* is present in the sites. Second, the orientations of the Chls in their binding pockets in LHCII-db and LHCII-ab were compared (Figure S5B in Supporting Information). For all Chls, the difference is small, indicating that the formyl group of Chl *d* does not induce additional steric hindrances or interactions that influence the position of the Chl within the protein complex.

To probe whether the presence of Chl *d* affects the protein structure of LHCII, we compared the equilibrated secondary structure of LHCII-db with that of LHCII-ab per protein domain (Figure S6A in Supporting Information). The types of secondary structures were assigned following the Dictionary for the Secondary Structure of Proteins (DSSP), in which each residue can be either a coil, β-sheet, β-bridge, bend, turn, α-helix, 3_{10}-helix, π-helix, or chain separator. As reported in Figure S6A in Supporting Information, we found that each protein domain of LHCII-db (protein domains listed in Figure S6D in Supporting Information) maintains the type of the secondary structure of LHCII-ab, indicating that binding of Chl *d* does not alter the folding architecture of LHCII. Binding of Chl *d* might, however, alter the flexibility of the complex. To assess whether this is the case, we computed the B-factors, which are a measure of the displacement of the atoms of each residue with respect to their average position per time unit and, as such, indicate how flexible/rigid the different regions are. The high similarity between the B-factors in LHCII-db and -ab (Figures S6C and S7 in Supporting Information) shows that the substitution of Chl *a* by Chl *d* has little or no effect on the flexibility of the protein, indicating that no additional conformational disorder to the complex is induced by Chl *d*.

LHCII-db Maintains an Excitonic Architecture. In LHCII and more in general, in all LHCs, the Chl−Chl interactions largely define the absorption spectrum of the complexes and determine their excitation dynamics. We have analyzed whether the excitonic structure of LHCII-ab is maintained in Chl *d*-containing LHCII by comparing the CD spectra of the two complexes. The CD spectrum of LHCII-ab (Figure 3A) shows the typical −/+/− feature with bands at 647, 662, and 680 nm in the Q_y-region.[33] The LHCII-db spectrum (Figure 3A) shows a similar pattern with bands at 645(−), 659(+), 684(+), and 702(−) nm, indicating that also the Chls *d* participate in excitonic interactions. Notably, the presence of a strong band at longer wavelengths in both complexes (680 nm for the LHCII-ab and 702 nm for LHCII-db) suggests that the cluster responsible for this band is preserved. The largest contribution to the red-most band in LHCII-ab originates from the CLA611−CLA612 pair, which is the terminal emitting site in LHCII.[16,33−35]

To analyze the interactions among Chls in LHCII-db in more detail, the average excitonic interactions for the most strongly coupled Chl pairs in LHCII[35] were computed on the MD trajectories and compared to those of LHCII-ab[31] (Figure 3B). These interaction energies were found to be similar in the two complexes, with the largest difference being 26.0 ± 14.4 cm^{-1} for the CLB606-CLA/D604 pair. These results indicate that the excitonic architecture in the LHCII is conserved upon the incorporation of Chl *d*.

Chl *d* Incorporation in LHCII Results in Efficient Light Harvesting. To probe the effect of Chl *d*-binding on the excited-state lifetime of LHCII, the fluorescence decay kinetics of LHCII-db were measured and compared to those of LHCII-ab. For both complexes, three lifetime components were needed to satisfactorily fit the fluorescence decay (Figure 3C, amplitudes and lifetimes are reported in the table in Figure 3D). The distribution of conformations in terms of fluorescence lifetime is virtually the same for both complexes: their decay is dominated by two nanosecond components, while the sub-nanosecond component has a relatively low amplitude. This shows that no additional quenching channels are created upon binding of Chl *d* to LHCII. The lifetimes associated with these conformations are even clearly longer in the case of the LHCII-db complex. Since the natural lifetime of Chl *d* in solution is very similar to that of Chl *a* (6.5 and 6.3 ns in pyridine, respectively[36]), this indicates that Chl *d* is quenched to a lesser extent in LHCII than Chl *a* is. In any case, the average lifetime for both complexes is long (>2 ns, Figure 3D). Such a long excited-state lifetime is crucial for efficient light-harvesting in the photosynthetic membrane.

LHCII-db Exhibits Fast Inter-Chl Energy Transfer. Numerous studies have elucidated the energy transfer pathways and timescales in the LHCII complex.[32,34,35,37−47] In these studies, inter-Chl excitation energy transfer (EET) proceeds with time constants ranging from 100 fs to a few picoseconds, depending on the pigment clusters involved. Förster resonance energy transfer theory provides a reasonable approximation to explain EET in the LHCs.[32] Since the overlap integral for Chl *b* and Chl *d* is smaller than that for Chl *b* and Chl *a*, it is expected that the energy transfer rates in the LHCII-db sample are somewhat slower than in the LHCII-ab complexes. To probe whether this is the case and to find out the consequences of the insertion of Chl *d* in LHCII for EET, we performed ultrafast transient absorption measurements. In these experiments, the pump was set at 642 nm to preferentially excite the Q_y band of Chl *b*.

By convoluting the individual Chl spectra obtained from the fit of the LHCII-db absorption spectrum (Figure 2E) with the laser pulse shape (modeled as a Gaussian centered at 642 nm with fwhm of 10 nm), we estimate an initial Chl *b*:Chl *d* excitation distribution of ∼70:30. Global analysis on the acquired 2D temporal spectral map allowed the identification of the principal EADS (Figure 4B) and DADS (Figure 4C). In Figure S2C in Supporting Information, a selection of time traces of the global fit is displayed alongside the corresponding measured traces.

In the first EADS (Figure 4B, black trace), which corresponds to the time zero spectrum, we observe bleaching signals in both the Chl *b* and Chl *d* absorption regions. By taking into account the difference in oscillator strength between Chl *b* and *d* (∼0.7:1), we calculated an initial excitation distribution of Chl *b*:Chl *d* of 72:28, which is consistent with the fitting of the absorption spectra. Two distinct bleaches can be observed in the Chl *b* region, at 643 and 649 nm, indicating that two (pools of) Chl *b* are initially excited. The initial Chl *d* bleach is quite broad, which suggests that also multiple (pools of) Chl *d* are excited. The first EADS evolves into the second one (Figure 4B, red trace) in 233 fs, showing EET from blue-to-red Chls *b* and significant transfer from Chl *b* to different Chl *d* pools, as suggested by the width of the Chl *d* peak. This transfer can be better visualized in the first DADS (Figure 4C, black trace) in the form of a negative

https://doi.org/10.1021/acs.biomac.1c00435
Biomacromolecules 2021, 22, 3313−3322

signal with minima at 643 and 649 nm and positive signals around 660 nm and 700 nm. In 1.5 ps, the second EADS evolves into the third one (Figure 4B, blue trace). In the second DADS (Figure 4C, red trace), the negative signal in the Chl *b* region and a broad positive signal, with a shoulder at 693 nm and a peak at 703 nm, indicate transfer from Chl *b* to spectrally distinct Chl *d* pools. The Chl *b* bleach is red-shifted with respect to the previous DADS, which indicates that EET transfer occurs mainly from the red Chls *b*. The fourth EADS (Figure 4B, pink trace) is formed within 8.8 ps and represents the slower step of the Chl *b* to Chl *d* transfer process and the equilibration between Chl *d* pools. Both processes are visible in the third DADS (Figure 4C, blue trace), in which there are two negative signals around 651 and 690 nm and a large positive peak at 705 nm. The remaining bleach at 705 nm in the fourth EADS (Figure 4B, pink trace) decays in 1.9 ns and forms a long-lived state (fifth EADS, Figure 4B, green trace), which can be attributed to Chl and Car triplets.[48] The fourth EADS (Figure 4B, pink trace) of 1.9 ns matches the time-resolved fluorescence data (see above and Figure 3C,D). Notably, two distinct Chl *d* pools exist, the bluer transferring slowly (EET completed in ∼9 ps, Figure 4C blue DADS) to the most-red one. This slow and blue pool of Chl *d* is reminiscent of the slow blue pool of Chls *a* observed in WT LHCII, which is associated with CLA604 and transfers to the CLA610−CLA611−CLA612 cluster.[34,35] Arguably, these binding sites are therefore occupied by Chl *d* in LHCII-db.

To put the LHCII-db EET kinetics into context, we have also performed TA measurements on the LHCII-ab complex under the same experimental conditions. The results of the global analysis of the pump−probe experiment on LHCII-ab are shown in Figure 4D−F. The time-zero spectrum (Figure 4E, black trace) shows an initial excitation distribution of Chl *b*:*a* of 75:25 (taking into account the oscillator strengths of Chl *b*:*a* of ∼0.7:1), which is comparable to the excitation distribution Chl *b*:*d* in the LHCII-db experiment. The identified components are consistent with previously reported kinetics of monomeric WT LHCII-ab complexes measured under similar experimental conditions.[44] Moreover, the EET steps are evidently similar to those of the LHCII-db complex: the first EET component (black trace in Figure 4F and 4C, respectively) show EET from a blue and red Chl *b* peaking at ∼641 and ∼648 nm to a broad Chl *a*/*d* band. The second component (red trace in Figure 4F and 4C, respectively) shows EET from a red Chl *b* peaking around 650 nm to Chl *a*/*d*. The third slow EET components (blue trace in Figure 4F and 4C, respectively) show EET from the remaining excitations on Chl *b* and from a blue Chl *a*/*d* band to the red terminal emitting the Chl *a*/*d* band. The fourth and fifth components (pink and green traces in Figure 4F and 4C, respectively) show the decay of the excited state of the terminal emitting Chl *a*/*d* and emergence of Car triplets.

Although the processes of the inter-Chl EET components for LHCII-db and LHCII-ab are similar, their corresponding rates are significantly smaller in LHCII-db: a time constant of 233 fs *versus* 108 fs, 1.5 ps *versus* 753 fs, and 8.8 ps *versus* 4.9 ps. One possible reason for the slowing down of the EET might be the larger energy gap between Chl *d* and Chl *b*, with respect to Chl *a* and Chl *b*. To check this hypothesis, the difference in FRET rates between LHCII-ab and LHCII-db (see text S2 in Supporting Information) was estimated on the basis of the distances and orientations of the pigments obtained from the simulations and the overlap integral calculated for the transfer between the different Chl types in the system. Overall, the Chl *b* → Chl *a* FRET rates in LHCII-ab are estimated to be on average 2.19 times faster than the corresponding Chl *b* → Chl *d* rates in LHCII-bd, while the Chl *a* → Chl *a* FRET rates are similar to the Chl *d* → Chl *d* rates. The Chl *b* → Chl *b* rates are also expected to be similar in both complexes. These results are in line with the lifetimes observed experimentally, where the larger differences are in the first and second component (233 *vs* 108 fs and 1.5 ps *vs* 753 fs), which are mainly due to Chl *b* to Chl *a*/*d* transfer, while the difference in the third component (8.8 *vs* 4.9 ps) is smaller, in agreement with the fact that it is dominated by the equilibration within the Chl *a*/*d* band.

CONCLUSIONS

This work demonstrates the functional integration of chlorophyll *d*, a far-red absorbing pigment present in some cyanobacteria, into LHCII, the main LHC of plants. We show that chlorophyll *d*-binding LHCII displays a strong absorption in the far-red while maintaining the functional architecture of the native complex, that is, (i) the protein structure is unaltered and would thus not affect the assembly of this protein in functional complexes in plants; (ii) the presence of chlorophyll *d* does not create quenchers, maintaining the high light-harvesting efficiency typical of LHCII; (iii) the terminal emitter is conserved, allowing potential efficient EET to the other complexes and its use for photochemistry. All arguments considered, the study opens the way for engineering plant LHCs capable of enhanced light harvesting in the far-red.

ASSOCIATED CONTENT

Supporting Information

The Supporting Information is available free of charge at https://pubs.acs.org/doi/10.1021/acs.biomac.1c00435.

Pigment extraction absorption spectrum fits of LHCII-ab and LHCII-db; transient absorption power studies of LHCII-db and LHCII-ab and selected time traces of LHCII-db and LHCII-ab; comparison of Chl *a* and Chl *d* absorption spectra in the solvent in the Q_y region; MD methodology; chlorophyll ligands; LHCII-ab emission spectra; RMSD evolution of MD replicas and chlorophyll orientations in the MD simulations; protein secondary structure, LHCII complex B-factors, chlorophyll-ligand distances and protein domains; chlorophyll B-factors; FRET calculation; and overlap functions (PDF)

AUTHOR INFORMATION

Corresponding Author

Roberta Croce − *Department of Physics and Astronomy and Institute for Lasers, Life and Biophotonics, Faculty of Sciences, VU University Amsterdam, 1081 HV Amsterdam, The Netherlands;* orcid.org/0000-0003-3469-834X; Email: r.croce@vu.nl

Authors

Eduard Elias − *Department of Physics and Astronomy and Institute for Lasers, Life and Biophotonics, Faculty of Sciences, VU University Amsterdam, 1081 HV Amsterdam, The Netherlands*

Nicoletta Liguori − *Department of Physics and Astronomy and Institute for Lasers, Life and Biophotonics, Faculty of*

Sciences, VU University Amsterdam, 1081 HV Amsterdam, The Netherlands; orcid.org/0000-0001-5695-4012

Yoshitaka Saga − *Department of Physics and Astronomy and Institute for Lasers, Life and Biophotonics, Faculty of Sciences, VU University Amsterdam, 1081 HV Amsterdam, The Netherlands; Department of Chemistry, Faculty of Science and Engineering, Kindai University, Higashi-Osaka 577-8502 Osaka, Japan;* orcid.org/0000-0001-7384-9169

Judith Schäfers − *Department of Physics and Astronomy and Institute for Lasers, Life and Biophotonics, Faculty of Sciences, VU University Amsterdam, 1081 HV Amsterdam, The Netherlands*

Complete contact information is available at: https://pubs.acs.org/10.1021/acs.biomac.1c00435

Author Contributions

[§]E.E. and N.L. contributed equally.

Author Contributions

Conceptualization, R.C.; methodology, E.E., Y.S., N.L., and R.C.; investigation, E.E., Y.S., and N.L.; resources, Y.S. and J.S.; data analysis, E.E. and N.L.; writing original draft, E.E., N.L., and R.C.; writing—review and editing, E.E., N.L., Y.S., J.S., and R.C.; supervision, N.L. and R.C.

Notes

The authors declare no competing financial interest.

■ ACKNOWLEDGMENTS

This work is supported by The Netherlands Organization for Scientific Research (NWO) *via* a TOP grant (to R.C.). N.L. was supported by a NWO Veni grant. Y.S. was supported by a JSPS KAKENHI grant (JP17KK0106). The MD simulations of LHCII-db were carried out on the Dutch national e-infrastructure with the support of SURF Cooperative through a NWO grant to N.L. and R.C. We are very grateful to Frank van Mourik for helping us build the pump−probe setup and to Vincenzo Mascoli for helpful discussion.

■ REFERENCES

(1) Zhu, X.-G.; Long, S. P.; Ort, D. R. Improving photosynthetic efficiency for greater yield. *Annu. Rev. Plant Biol.* **2010**, *61*, 235−261.
(2) Croce, R.; van Amerongen, H. Natural strategies for photosynthetic light harvesting. *Nat. Chem. Biol.* **2014**, *10*, 492−501.
(3) Ort, D. R.; Merchant, S. S.; Alric, J.; Barkan, A.; Blankenship, R. E.; Bock, R.; Croce, R.; Hanson, M. R.; Hibberd, J. M.; Long, S. P.; Moore, T. A.; Moroney, J.; Niyogi, K. K.; Parry, M. A. J.; Peralta-Yahya, P. P.; Prince, R. C.; Redding, K. E.; Spalding, M. H.; van Wijk, K. J.; Vermaas, W. F. J.; von Caemmerer, S.; Weber, A. P. M.; Yeates, T. O.; Yuan, J. S.; Zhu, X. G. Redesigning photosynthesis to sustainably meet global food and bioenergy demand. *Proc. Natl. Acad. Sci. U.S.A.* **2015**, *112*, 8529−8536.
(4) Mirkovic, T.; Ostroumov, E. E.; Anna, J. M.; van Grondelle, R.; Govindjee; Scholes, G. D. Light absorption and energy transfer in the antenna complexes of photosynthetic organisms. *Chem. Rev.* **2017**, *117*, 249−293.
(5) Liu, Z.; Yan, H.; Wang, K.; Kuang, T.; Zhang, J.; Gui, L.; An, X.; Chang, W. Crystal structure of spinach major light-harvesting complex at 2.72 Å resolution. *Nature* **2004**, *428*, 287−292.
(6) Gundlach, K.; Werwie, M.; Wiegand, S.; Paulsen, H. Filling the ″green gap″ of the major light-harvesting chlorophyll a/b complex by covalent attachment of Rhodamine Red. *Biochim. Biophys. Acta, Bioenerg.* **2009**, *1787*, 1499−1504.
(7) Hancock, A. M.; Meredith, S. A.; Connell, S. D.; Jeuken, L. J. C.; Adams, P. G. Proteoliposomes as energy transferring nanomaterials: Enhancing the spectral range of light-harvesting proteins using lipid-linked chromophores. *Nanoscale* **2019**, *11*, 16284−16292.
(8) Chen, L.; Liu, C.; Hu, R.; Feng, J.; Wang, S.; Li, S.; Yang, C.; Yang, G. Two photon absorption energy transfer in the light-harvesting complex of photosystem II (LHC-II) modified with organic boron dye. *Spectrochim. Acta, Part A* **2014**, *128*, 295−299.
(9) Chen, M.; Schliep, M.; Willows, R. D.; Cai, Z.-L.; Neilan, B. A.; Scheer, H. A Red-Shifted Chlorophyll. *Science* **2010**, *329*, 1318−1319.
(10) Gan, F.; Shen, G.; Bryant, D. Occurrence of Far-Red Light Photoacclimation (FaRLiP) in Diverse Cyanobacteria. *Life* **2014**, *5*, 4−24.
(11) Chen, M.; Blankenship, R. E. Expanding the solar spectrum used by photosynthesis. *Trends Plant Sci.* **2011**, *16*, 427−431.
(12) Mielke, S. P.; Kiang, N. Y.; Blankenship, R. E.; Gunner, M. R.; Mauzerall, D. Efficiency of photosynthesis in a Chl d-utilizing cyanobacterium is comparable to or higher than that in Chl a-utilizing oxygenic species. *Biochim. Biophys. Acta, Bioenerg.* **2011**, *1807*, 1231−1236.
(13) Loughlin, P.; Lin, Y.; Chen, M. Chlorophyll d and Acaryochloris marina: current status. *Photosynth. Res.* **2013**, *116*, 277−293.
(14) Chen, M. Chlorophylls d and f: Synthesis, occurrence, light-harvesting, and pigment organization in chlorophyll-binding protein complexes. *Adv. Bot. Res.*; Grimm, B., Ed.; Academic Press, 2019; Vol. *90*, pp 121−139.
(15) Chen, M.; Willows, R. D.; Blankenship, R. E. Gene constructs comprising nucleic acids that modulate chlorophyll biosynthesis and uses thereof. WO2011143716, 2011.
(16) Remelli, R.; Varotto, C.; Sandonà, D.; Croce, R.; Bassi, R. Chlorophyll Binding to Monomeric Light-harvesting Complex. *J. Biol. Chem.* **1999**, *274*, 33510−33521.
(17) Giuffra, E.; Cugini, D.; Croce, R.; Bassi, R. Reconstitution and pigment-binding properties of recombinant CP29. *Eur. J. Biochem.* **1996**, *238*, 112−120.
(18) Hobe, S.; Fey, H.; Rogl, H.; Paulsen, H. Determination of relative chlorophyll binding affinities in the major light-harvesting chlorophyll a/b complex. *J. Biol. Chem.* **2003**, *278*, 5912−5919.
(19) Eggink, L. L.; Hoober, J. K. Chlorophyll binding to peptide maquettes containing a retention motif. *J. Biol. Chem.* **2000**, *275*, 9087−9090.
(20) Chen, M.; Cai, Z.-L. Theoretical study on the thermodynamic properties of chlorophyll d-peptides coordinating ligand. *Biochim. Biophys. Acta, Bioenerg.* **2007**, *1767*, 603−609.
(21) Natali, A.; Roy, L. M.; Croce, R. In Vitro Reconstitution of Light-harvesting Complexes of Plants and Green Algae. *J. Visualized Exp.* **2014**, *92*, No. e51852.
(22) Saga, Y.; Yamashita, M.; Imanishi, M.; Kimura, Y. Reconstitution of chlorophyll d into the bacterial photosynthetic light-harvesting protein LH2. *Chem. Lett.* **2018**, *47*, 1071−1074.
(23) Croce, R.; Canino, G.; Ros, F.; Bassi, R. Chromophore Organization in the Higher-Plant Photosystem II Antenna Protein CP26. *Biochemistry* **2002**, *41*, 7334−7343.
(24) van Oort, B.; Amunts, A.; Borst, J. W.; van Hoek, A.; Nelson, N.; van Amerongen, H.; Croce, R. Picosecond Fluorescence of Intact and Dissolved PSI-LHCI Crystals. *Biophys. J.* **2008**, *95*, 5851−5861.
(25) Digris, A. V.; Novikov, E. G.; Skakun, V. V.; Apanasovich, V. V. Global analysis of time-resolved fluorescence data. *Fluorescence Spectroscopy and Microscopy. Methods in Molecular Biology (Methods and Protocols)*; Engelborghs, Y., Visser, A., Eds.; Humana Press Inc., 2014; Vol. *1076*, pp 257−277.
(26) Stahl, A. D.; Di Donato, M.; van Stokkum, I.; van Grondelle, R.; Groot, M. L. A Femtosecond Visible/Visible and Visible/Mid-Infrared Transient Absorption Study of the Light Harvesting Complex II. *Biophys. J.* **2009**, *97*, 3215−3223.
(27) van Stokkum, I. H. M.; Larsen, D. S.; van Grondelle, R. Global and target analysis of time-resolved spectra. *Biochim. Biophys. Acta, Bioenerg.* **2004**, *1657*, 82−104.

(28) Snellenburg, J.; Laptenok, S.; Seger, R.; Mullen, K.; van Stokkum, I. H. M. Glotaran: A Java-based graphical user interface for the R package TIMP. *J. Stat. Softw.* **2012**, *49*, 1−22.
(29) Cinque, G.; Croce, R.; Bassi, R. Absorption spectra of chlorophyll a and b in Lhcb protein environment. *Photosynth. Res.* **2000**, *64*, 233−242.
(30) van der Spoel, D.; Lindahl, E.; Hess, B.; Groenhof, G.; Mark, A. E.; Berendsen, H. J. C. GROMACS: Fast, flexible, and free. *J. Comput. Chem.* **2005**, *26*, 1701−1718.
(31) Liguori, N.; Periole, X.; Marrink, S. J.; Croce, R. From light-harvesting to photoprotection: structural basis of the dynamic switch of the major antenna complex of plants (LHCII). *Sci. Rep.* **2015**, *5*, 15661.
(32) van Amerongen, H.; van Grondelle, R. Understanding the energy transfer function of LHCII, the major light-harvesting complex of green plants. *J. Phys. Chem. B* **2001**, *105*, 604−617.
(33) Georgakopoulou, S.; van der Zwan, G.; Bassi, R.; van Grondelle, R.; van Amerongen, H.; Croce, R. Understanding the Changes in the Circular Dichroism of Light Harvesting Complex II upon Varying Its Pigment Composition and Organization. *Biochemistry* **2007**, *46*, 4745−4754.
(34) Novoderezhkin, V.; Marin, A.; van Grondelle, R. Intra- and inter-monomeric transfers in the light harvesting LHCII complex: the Redfield-Förster picture. *Phys. Chem. Chem. Phys.* **2011**, *13*, 17093.
(35) Novoderezhkin, V. I.; Palacios, M. A.; van Amerongen, H.; van Grondelle, R. Excitation Dynamics in the LHCII Complex of Higher Plants: Modeling Based on the 2.72 Å Crystal Structure. *J. Phys. Chem. A* **2005**, *109*, 10493−10504.
(36) Swainsbury, D. J. K.; Faries, K. M.; Niedzwiedzki, D. M.; Martin, E. C.; Flinders, A. J.; Canniffe, D. P.; Shen, G.; Bryant, D. A.; Kirmaier, C.; Holten, D.; Hunter, C. N. Engineering of B800 bacteriochlorophyll binding site specificity in the Rhodobacter sphaeroides LH2 antenna. *Biochim. Biophys. Acta, Bioenerg.* **2019**, *1860*, 209−223.
(37) Pålsson, L. O.; Spangfort, M. D.; Gulbinas, V.; Gillbro, T. Ultrafast chlorophyll *b*-chlorophyll *a* excitation energy transfer in the isolated light harvesting complex, LHC II, of green plants. *FEBS Lett* **1994**, *339*, 134−138.
(38) Bittner, T.; Irrgang, K.-D.; Renger, G.; Wasielewski, M. R. Ultrafast excitation energy transfer and exciton-exciton annihilation processes in isolated light harvesting complexes of photosystem II (LHC II) from spinach. *J. Phys. Chem.* **1994**, *98*, 11821−11826.
(39) Salverda, J. M.; Vengris, M.; Krueger, B. P.; Scholes, G. D.; Czarnoleski, A. R.; Novoderezhkin, V.; Amerongen, H. v.; Grondelle, R. v. Energy transfer in light-harvesting complexes LHCII and CP29 of spinach studied with three pulse echo peak shift and transient grating. *Biophys. J.* **2003**, *84*, 450−465.
(40) Gradinaru, C. C.; Van Stokkum, I. H. M.; Pascal, A. A.; van Grondelle, R.; van Amerongen, H. Identifying the Pathways of Energy Transfer between Carotenoids and Chlorophylls in LHCII and CP29. A Multicolor, Femtosecond Pump−Probe Study. *J. Phys. Chem. B* **2000**, *104*, 9330−9342.
(41) Holt, N. E.; Kennis, J. T. M.; Dall'Osto, L.; Bassi, R.; Fleming, G. R. Carotenoid to chlorophyll energy transfer in light harvesting complex II from Arabidopsis thaliana probed by femtosecond fluorescence upconversion. *Chem. Phys. Lett.* **2003**, *379*, 305−313.
(42) Kwa, S. L. S.; van Amerongen, H.; Lin, S.; Dekker, J. P.; van Grondelle, R.; Struve, W. S. Ultrafast energy transfer in LHC-II trimers from the Chl *a/b* light-harvesting antenna of Photosystem II. *Biochim. Biophys. Acta, Bioenerg.* **1992**, *1102*, 202−212.
(43) Croce, R.; Müller, M. G.; Bassi, R.; Holzwarth, A. R. Carotenoid-to-Chlorophyll Energy Transfer in Recombinant Major Light-Harvesting Complex (LHCII) of Higher Plants. I. Femtosecond Transient Absorption Measurements. *Biophys. J.* **2001**, *80*, 901−915.
(44) Palacios, M. A.; Standfuss, J.; Vengris, M.; van Oort, B. F.; van Stokkum, I. H. M.; Kühlbrandt, W.; van Amerongen, H.; van Grondelle, R. A comparison of the three isoforms of the light-harvesting complex II using transient absorption and time-resolved fluorescence measurements. *Photosynth. Res.* **2006**, *88*, 269−285.
(45) Kleima, F. J.; Gradinaru, C. C.; Calkoen, F.; van Stokkum, I. H. M.; van Grondelle, R.; van Amerongen, H. Energy transfer in LHCII monomers at 77K studied by sub-picosecond transient absorption spectroscopy. *Biochemistry* **1997**, *36*, 15262−15268.
(46) Visser, H. M.; Kleima, F. J.; van Stokkum, I. H. M.; van Grondelle, R.; van Amerongen, H. Probing the many energy-transfer processes in the photosynthetic light-harvesting complex II at 77 K using energy-selective sub-picosecond transient absorption spectroscopy. *Chem. Phys.* **1996**, *210*, 297−312.
(47) Connelly, J. P.; Müller, M. G.; Bassi, R.; Croce, R.; Holzwarth, A. R. Femtosecond Transient Absorption Study of Carotenoid to Chlorophyll Energy Transfer in the Light-Harvesting Complex II of Photosystem II. *Biochemistry* **1997**, *36*, 281−287.
(48) Mozzo, M.; Dall'Osto, L.; Hienerwadel, R.; Bassi, R.; Croce, R. Photoprotection in the Antenna Complexes of Photosystem II. *J. Biol. Chem.* **2008**, *283*, 6184−6192.

https://doi.org/10.1021/acs.biomac.1c00435
Biomacromolecules 2021, 22, 3313−3322